NATIONAL ADVISORY COMMITTEE FOR AERONAUTICS

TECHNICAL MEMORANDUM

No. 1159

WIND-TUNNEL MEASUREMENTS ON THE HENSCHEL MISSILE "ZITTERROCHEN" IN SUBSONIC AND SUPERSONIC VELOCITIES

By Weber and Kehl

Translation
"Windkanalmessungen am Henschel-Gerät 'Zitterrochen' bei Unter- und Überschallgeschwindigkeiten"

Deutsche Luftfahrtforschung, Untersuchungen und Mitteilungen Nr. 3122

and

WIND-TUNNEL MEASUREMENTS ON THE WING OF THE HENSCHEL MISSILE "ZITTERROCHEN" IN SUBSONIC AND SUPERSONIC VELOCITIES

By Kehl

Translation
"Windkanalmessungen am Flügel des Henschelgerätes 'Zitterrochen' bei Unter- und Überschallgeschwindigkeiten"

Deutsche Luftfahrtforschung, Untersuchungen und Mitteilungen Nr. 3161

Washington

April 1948

NATIONAL ADVISORY COMMITTEE FOR AERONAUTICS

TECHNICAL MEMORANDUM NO. 1159

WIND-TUNNEL MEASUREMENTS ON THE HENSCHEL MISSILE "ZITTERROCHEN"[1] IN SUBSONIC AND SUPERSONIC VELOCITIES*

By Weber and Kehl

Abstract: At the request of the Henschel Aircraft Works, A. G. Berlin, three models of the missile "Zitterrochen" were investigated at subsonic velocities (open jet 215-millimeter diameter) and at supersonic velocities (open jet 110 by 130 millimeters) in order to determine the effect of various wing forms on the air forces and moments. Three-component measurements were taken, and one model was also investigated with deflected control plates.

Outline: I. Relations and Definitions

II. Description of Model and Measured Results

I. RELATIONS AND DEFINITIONS

A lift, component of the air forces perpendicular to the direction of flow, kilograms

W drag, component of the air forces in the direction of flow, kilograms

---

*"Windkanalmessungen am Henschel-Gerät 'Zitterrochen' bei Unter- und Überschallgeschwindigkeiten." Zentrale für wissenschaftliches Berichtswesen der Luftfahrtforschung des Generalluftzeugmeisters (ZWB) - Berlin-Adlershof, Untersuchungen und Mitteilungen Nr. 3122. ~~Oct. 7,~~ July 10, 1944.

[1]Literally "trembling ray." (This type of ray is that which lives in the ocean. Presumably the name originated because of the triangular shape of the ray.)

M_o moment, referred to the projectile body, kilogram-meters

f distance of the pressure point from the rear edge of the projectile, meters

D caliber of the projectile body, meters

F cross-sectional area of the projectile, meters^2 $\frac{D^2}{4\pi}$

ρ density of air (kg sec^2 m^{-4})

v stream velocity (m sec^{-1})

a velocity of sound (m sec^{-1})

α angle of attack, degrees

M Mach number (v/a)

c_a lift coefficient $\left(\frac{A}{\frac{\rho}{2}v^2F}\right)$

c_w drag coefficient $\left(\frac{W}{\frac{\rho}{2}v^2F}\right)$

c_{m_o} moment coefficient $\left(\frac{M_o}{\frac{\rho}{2}v^2FD}\right)$

II. DESCRIPTION OF MODEL AND MEASURED RESULTS

The models tested are illustrated in figures 1 to 3. They differ only in wing form; the projectile bodies are all the same. The wings have about the same area, but the aspect ratios are different (2.0, 1.0, 0.5) and the thickness ratios are different. The profiles of the wing are the same all along the span. For the measurements at $M < 1$ a model length of 200 millimeters and for $M > 1$ a model length of 80 millimeters was chosen

(corresponding to projectile diameters of 20.4 and 8.2 millimeters, respectively). The Reynolds numbers based on the length of the body of the projectile are

R	M
2×10^6	0.5×10^6
3.1	.9
1.3	1.5
1.1	2.0

The models were supported at the stern by an inclined strut. At subsonic velocities (open jet 215-millimeter diameter) measurements were conducted at M = 0.5, 0.8, 0.85, and 0.9. Tunnel corrections were not used. At supersonic velocities measurements were taken at M = 1.45 and 1.99. The angle of attack was varied from 0° to 10°.

In figures 4 to 10 the lift coefficient c_a, drag coefficient c_w, moment coefficient c_{m_o}, and the position of the pressure point $\frac{f}{D} = \frac{c_{m_o}}{c_n}$ ($c_n = c_a \cos \alpha + c_w \sin \alpha$) are given for the three different models at constant Mach numbers, so that the effect of various wing forms is visible. With increasing aspect ratio the values $dc_a/d\alpha$ and $dc_{m_o}/d\alpha$ increased for all Mach numbers investigated; furthermore, the drag coefficient also increased, particularly at large angles of attack in the subsonic region and on the other hand, even at $\alpha = 0$ for the supersonic region on account of the larger thickness ratios.

The pressure point shifted forward at all velocities as the aspect ratio was increased.

In figures 11 to 13 the same measured results are presented against Mach number. In the subsonic region the lift coefficients show an increasing trend with increasing Mach number in the sense of Prandtl's equation. No significant decrease in the lift coefficient was observed when approaching the velocity of sound over the range of velocities investigated; however, it is to be noted that on account of not observing the jet corrections the results at M = 0.9 are uncertain. Over the range

of supersonic velocities investigated the lift coefficients for the same angle of attack are of the same magnitude as in the subsonic region.

The drag coefficient at small angles of attack slightly decreases with increasing Mach number, which is explained by the Reynolds number effect on the flow about the wing. At $M > 1$ the drag coefficients are naturally higher, since even in a frictionless fluid a drag would result on account of the finite thickness.

The pressure point of forms ZR 2.0 and ZR 1.0 are independent of the angle of attack and in the subsonic region it lies about 0.2 D closer to the projectile point than at supersonic velocities. For the form ZR 0.5 a shift of the pressure point forward was observed as the angle of attack was decreased.

In order to obtain a general idea of the effectiveness of control plates, the model ZR 2.0 was tested with deflected control plates at $M = 0.7$, 0.85, 1.45, and 1.99. The measurements of the deflected control plates are given in figure 1. In figures 14 to 17 the measured results are presented against angle of attack. As was to be expected, the effectiveness of the control plates was less in the supersonic regions than at velocities below that of sound.

In figures 4 to 17, again it is pointed out that the curves of the force and moment coefficients use as a reference area the projectile cross section $(\pi/4)D^2$ and as a reference length the caliber D, as is generally done for projectiles.

Translated by Chance-Vought
Aircraft Corporation

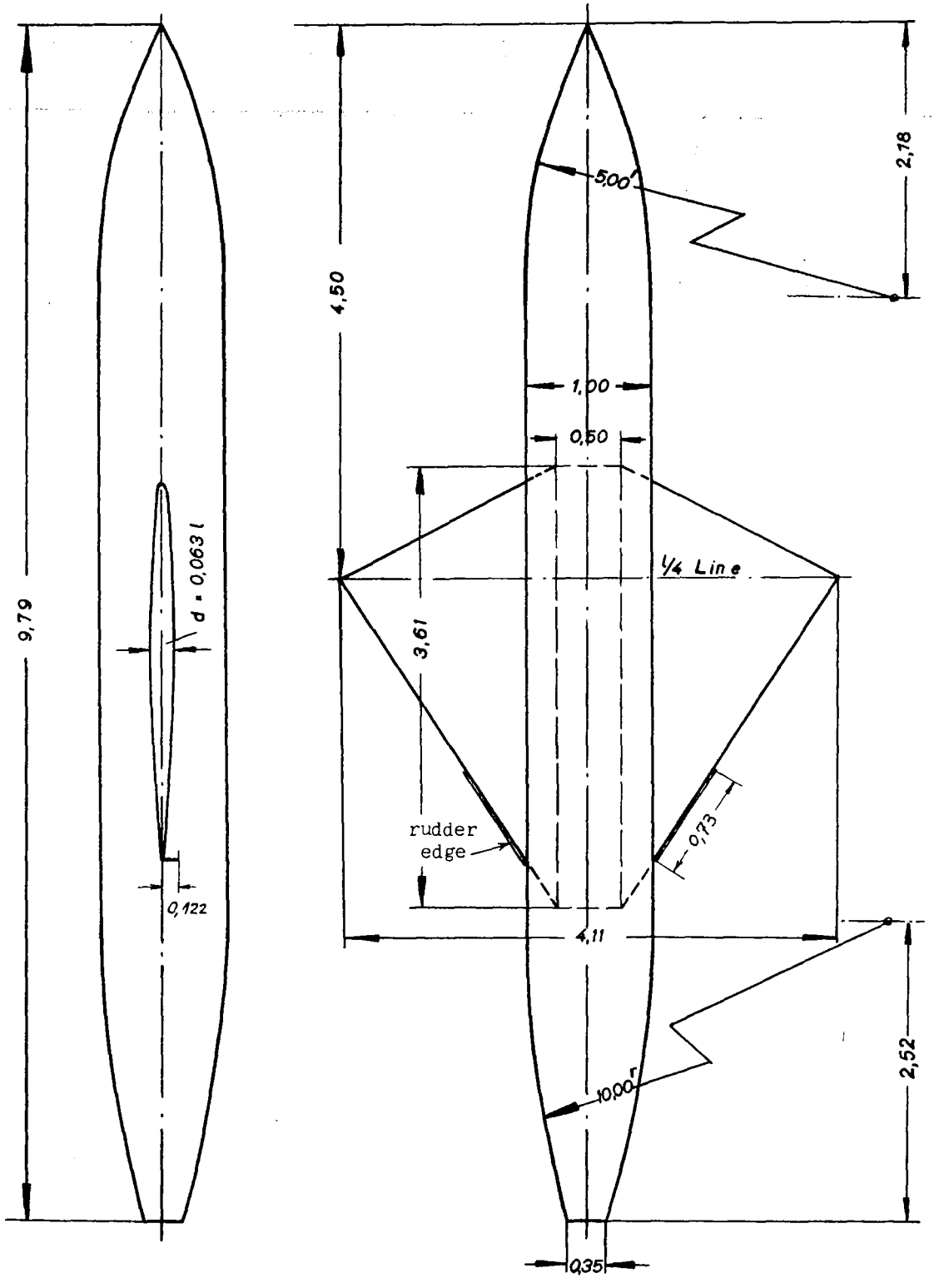

Figure 1.- Model ZR-2.0 according to drawing No. FA-SK 280.

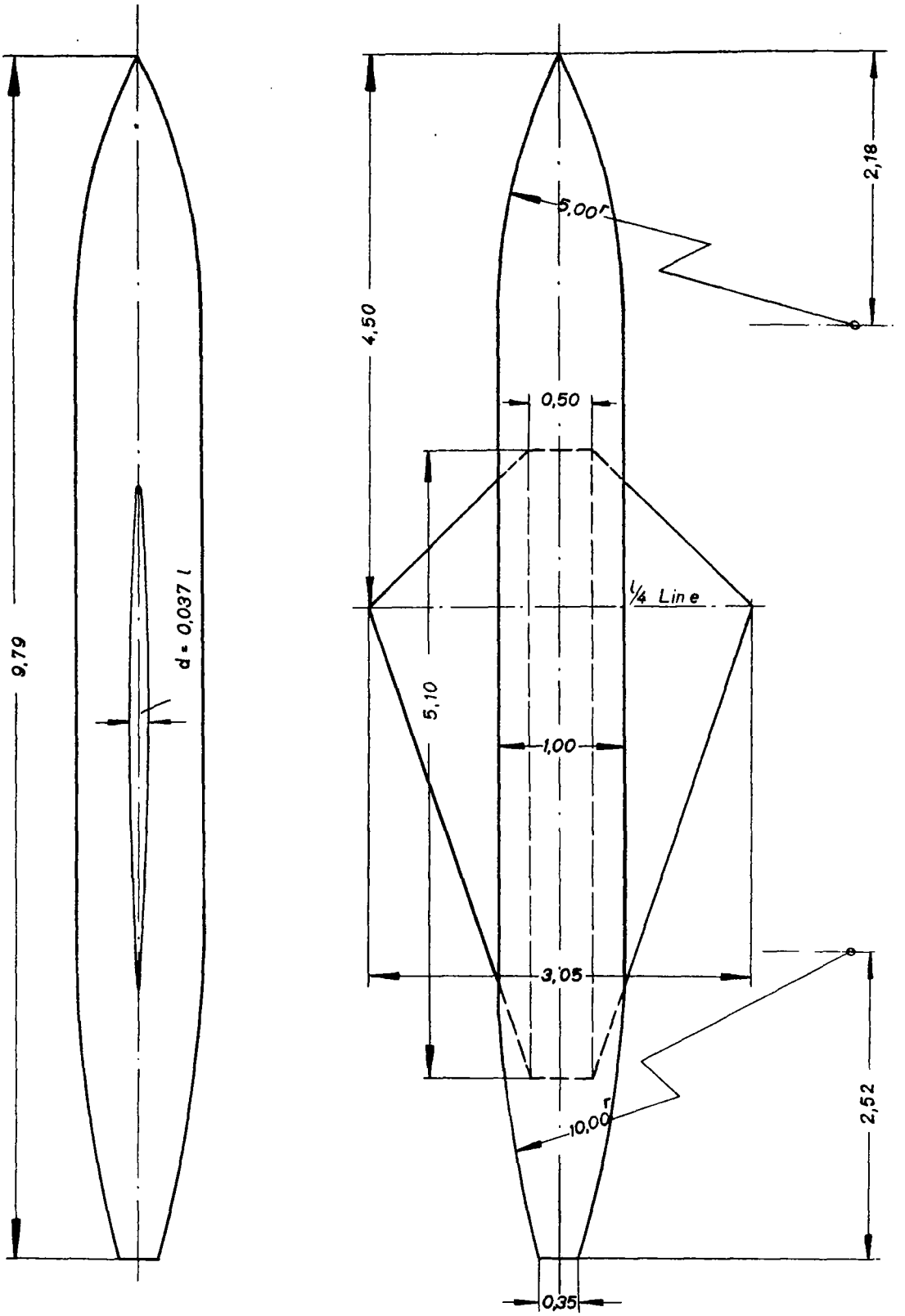

Figure 2.- Model ZR-1.0 according to drawing No. FA-SK 279.

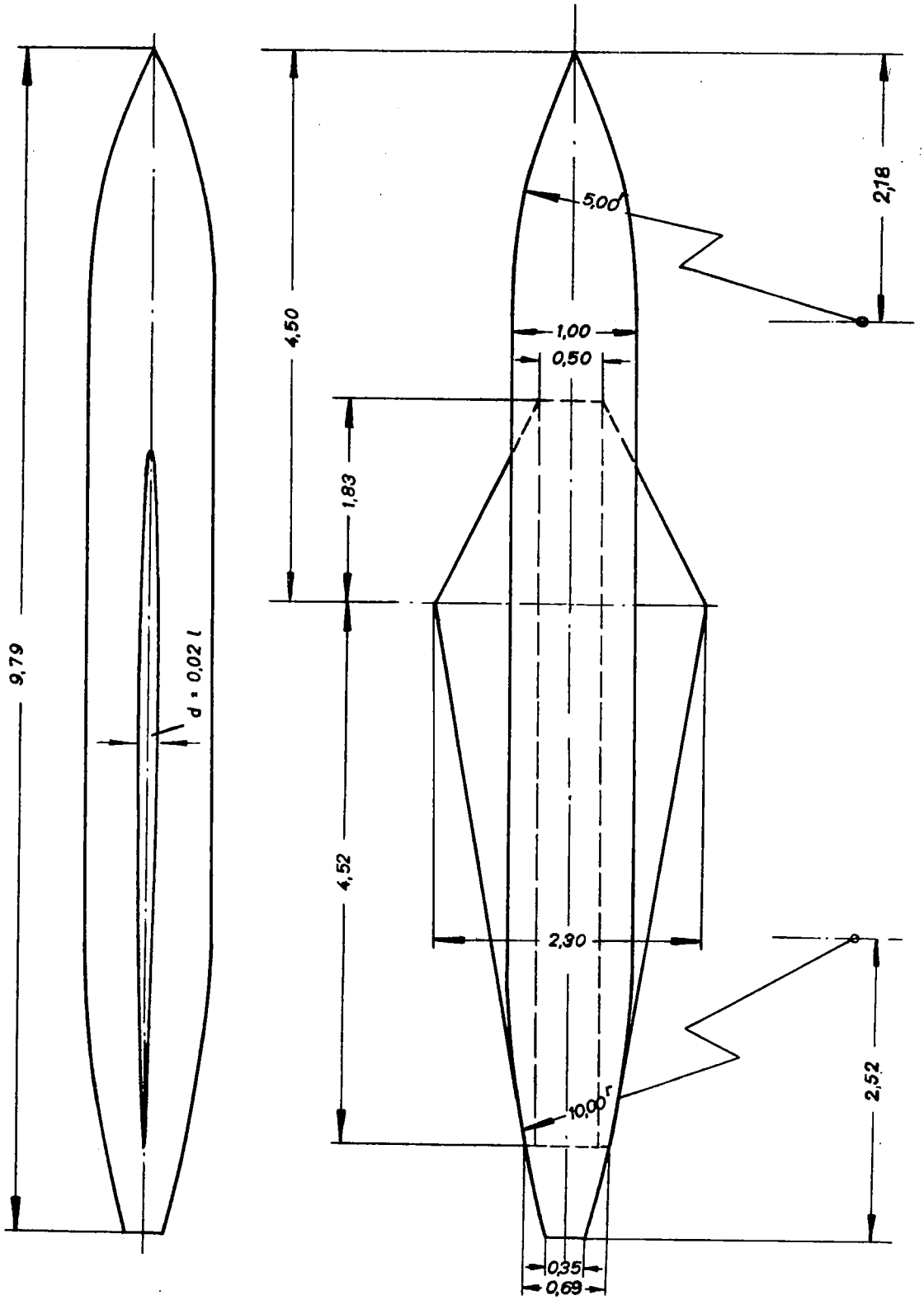

Figure 3.- Model ZR-0.5 according to drawing No. FA-SK 278.

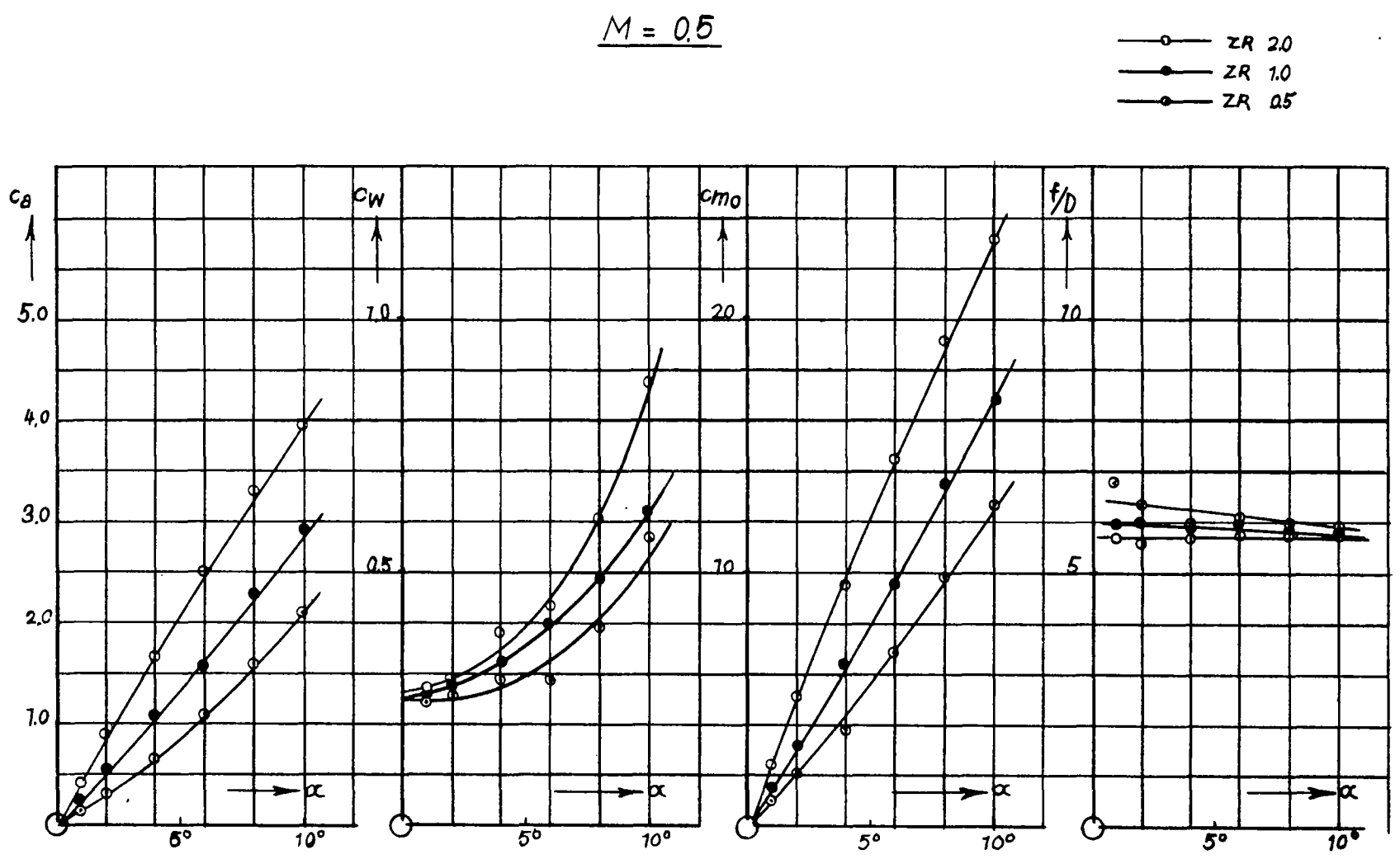

Figure 4.

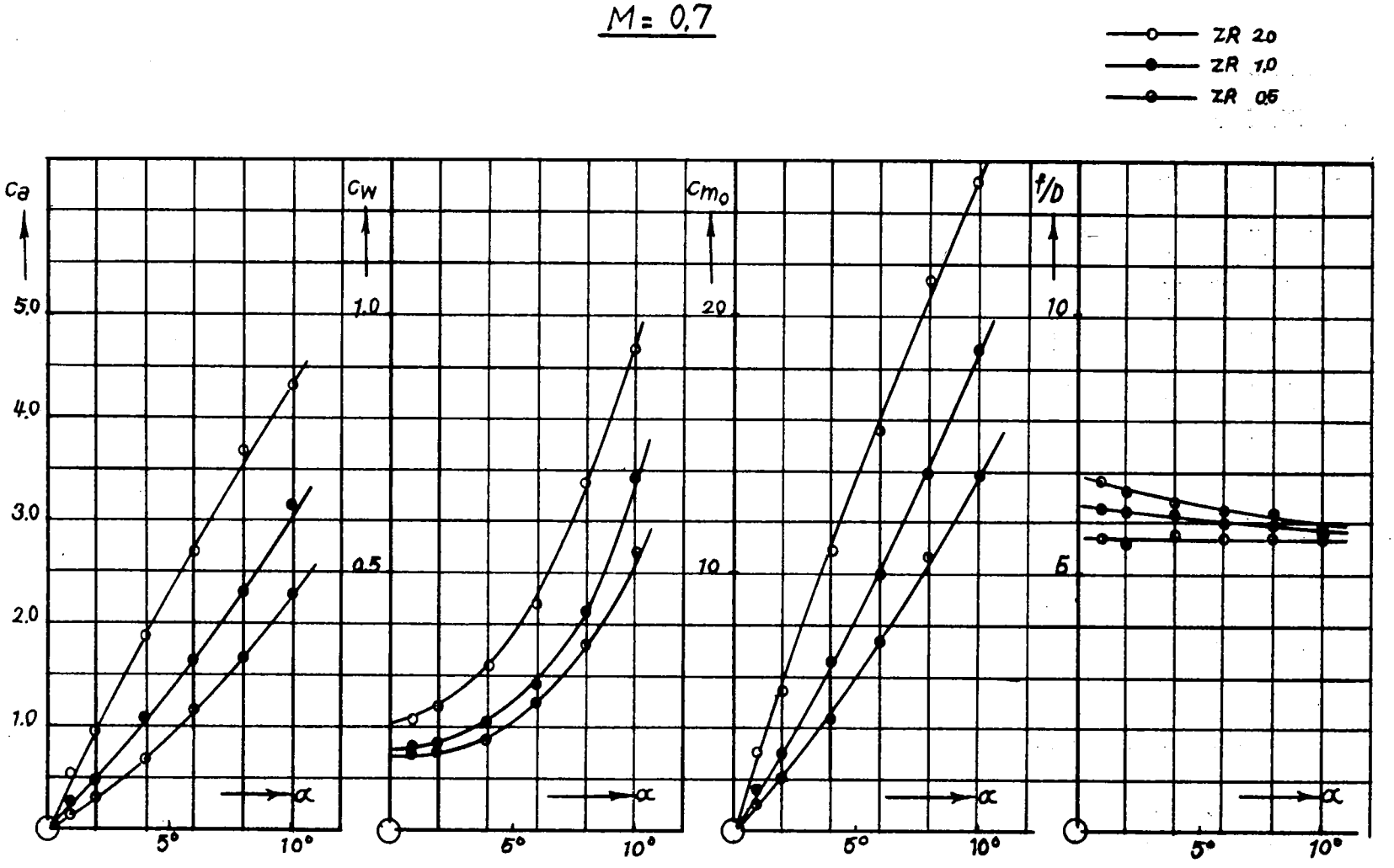

Figure 5.

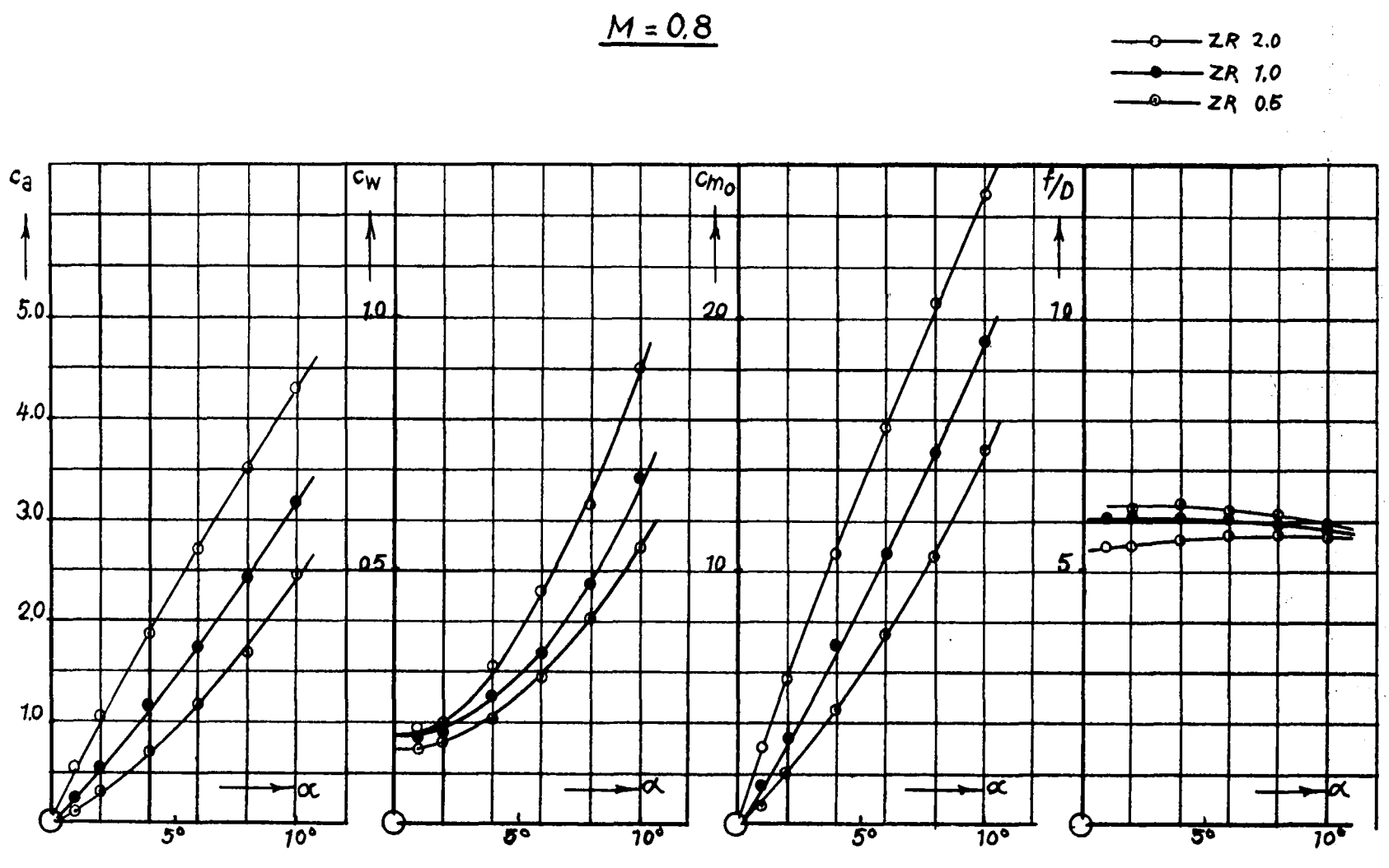

Figure 6.

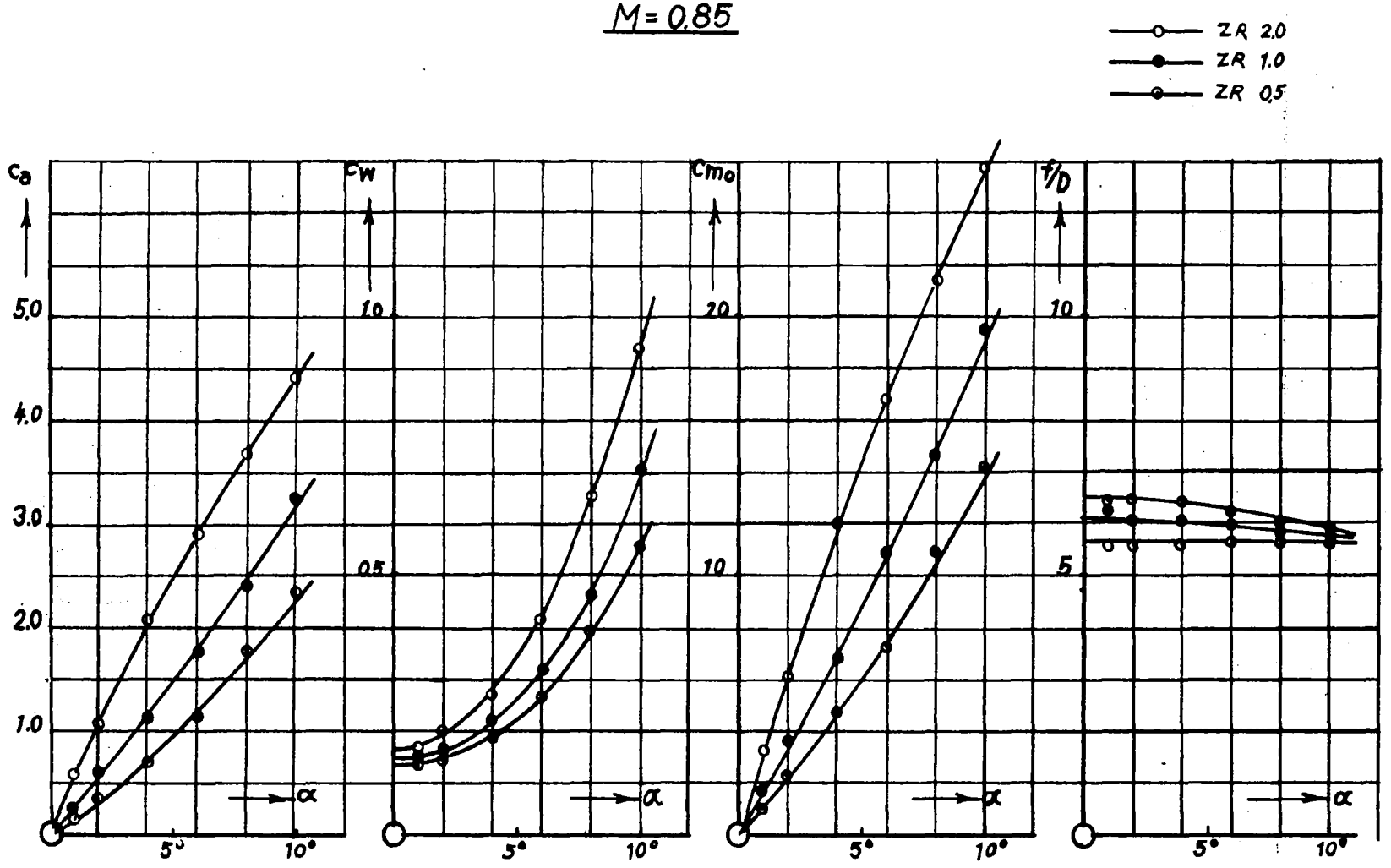
M = 0.85
ZR 2.0
ZR 1.0
ZR 0.5
C_a
5.0
4.0
3.0
2.0
1.0
C_w
.10
.05
C_{mo}
.20
.10
f/D
10
5
α
5°
10°

Figure 7.

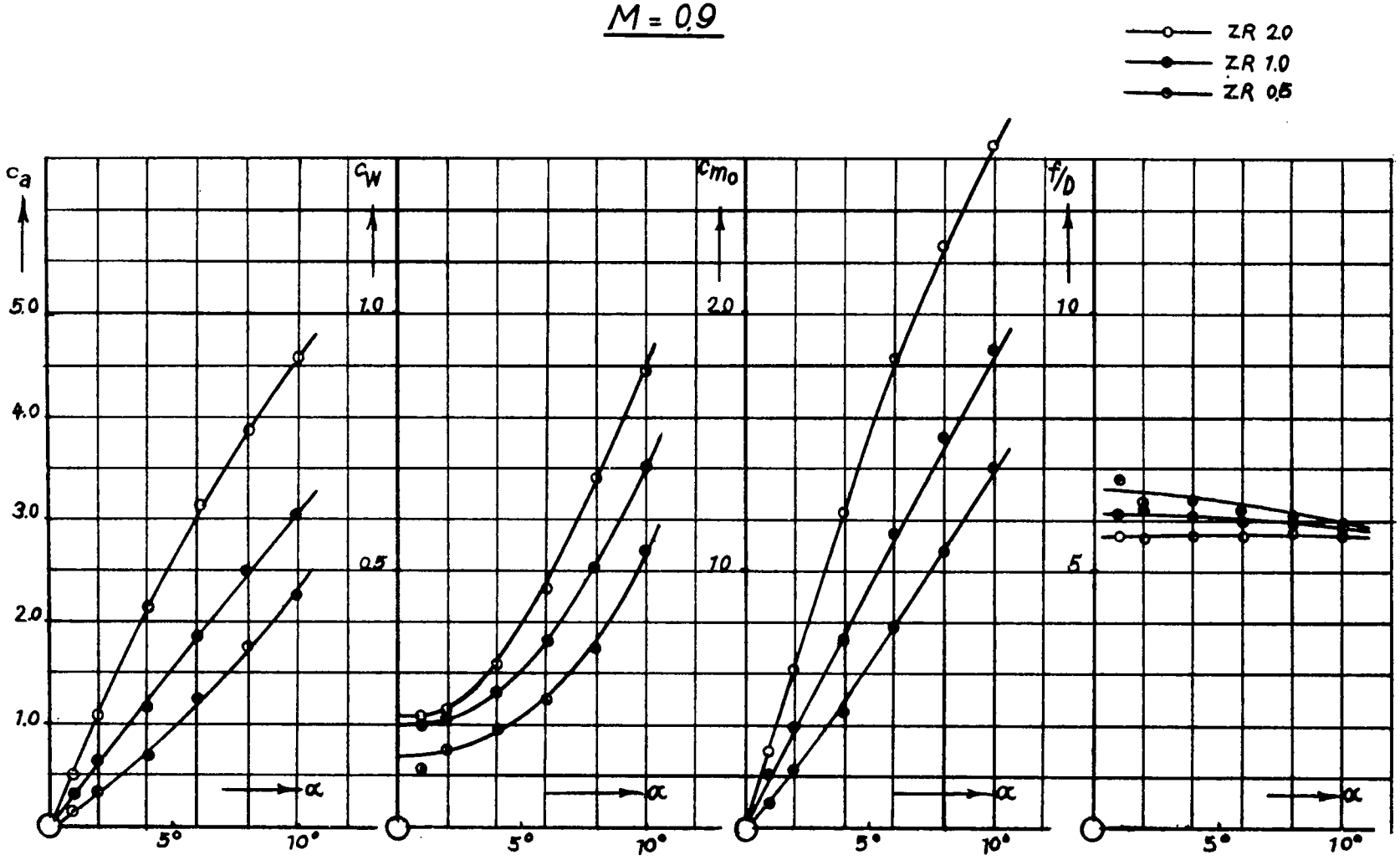

Figure 8.

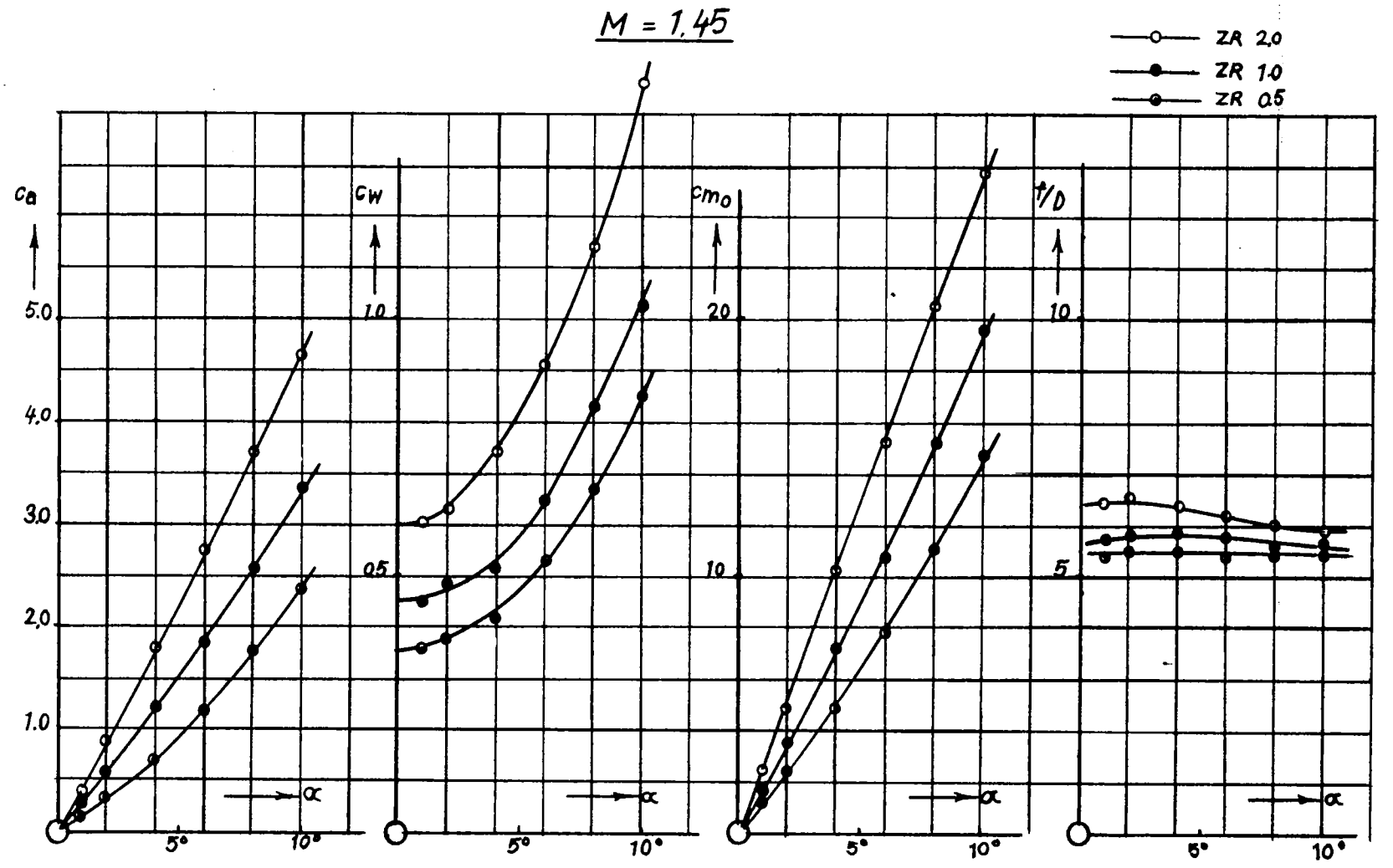
M = 1.45
ZR 2.0
ZR 1.0
ZR 0.5
c_a
5.0
4.0
3.0
2.0
1.0
c_w
1.0
0.5
c_{m_0}
20
10
T/D
10
5
α
5°
10°

Figure 9.

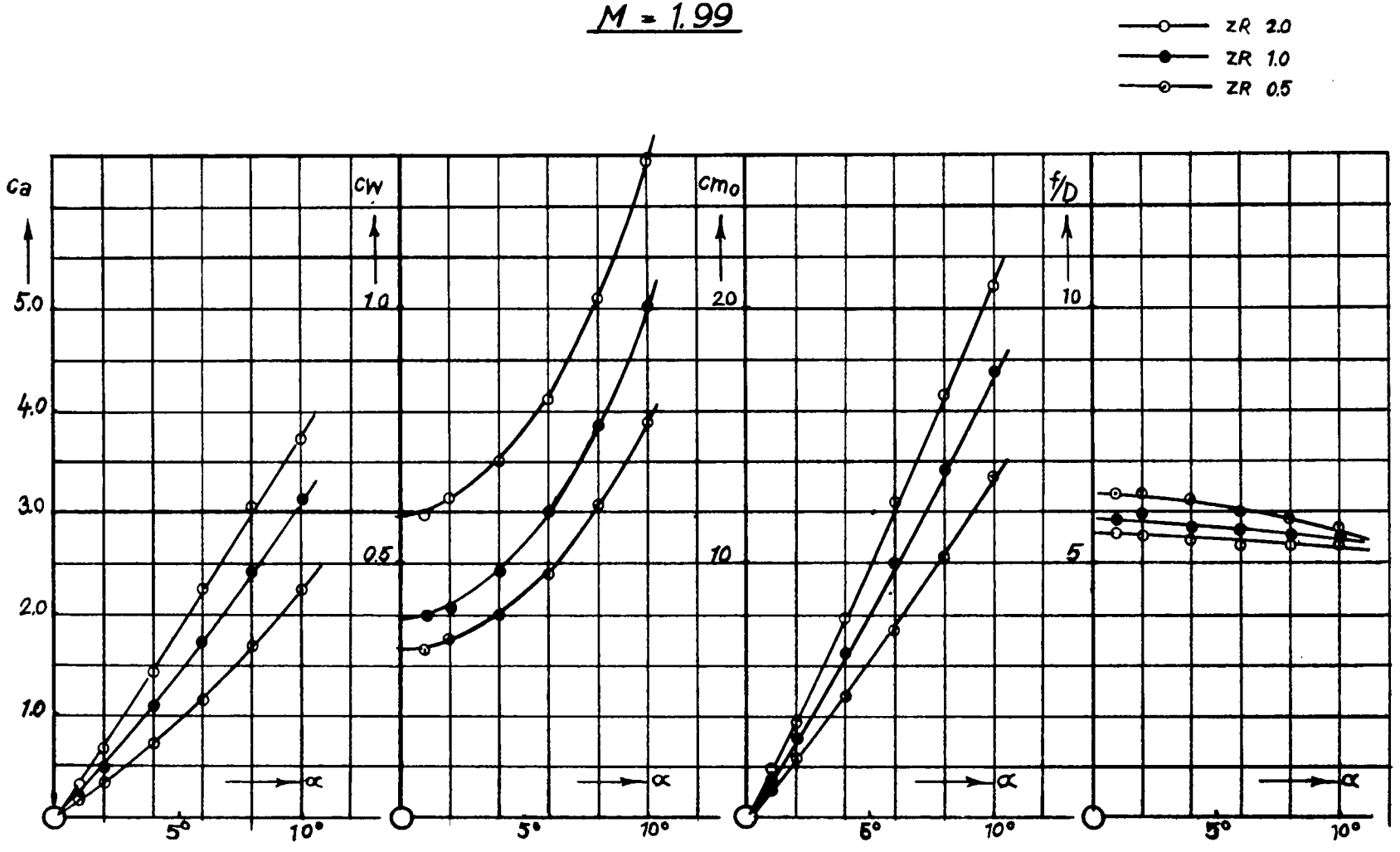
M = 1.99
ZR 2.0
ZR 1.0
ZR 0.5
Ca
5.0
4.0
3.0
2.0
1.0
Cw
1.0
0.5
Cmo
20
10
f/D
10
5
α
5°
10°

Figure 10.

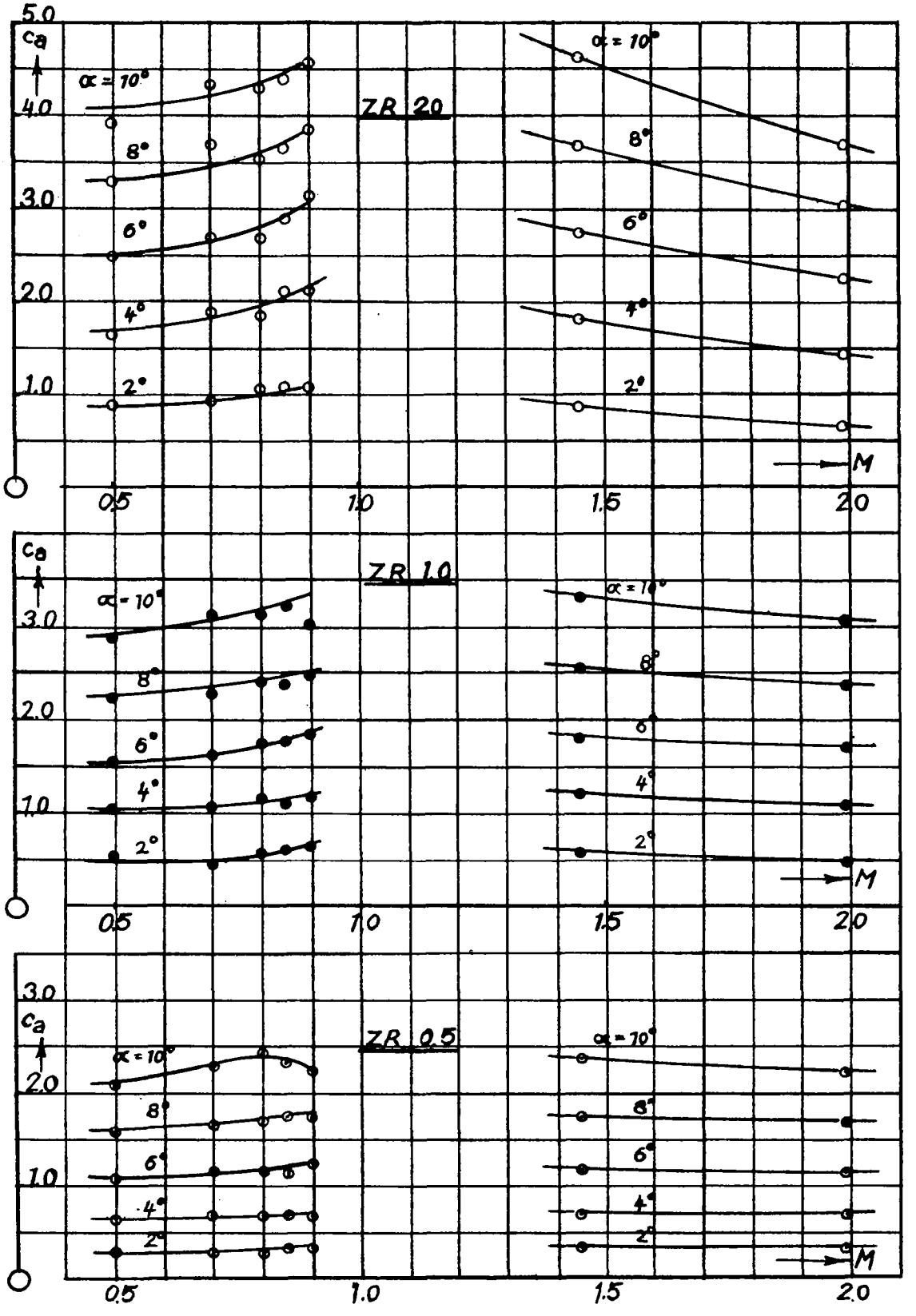

Figure 11.- Lift coefficients.

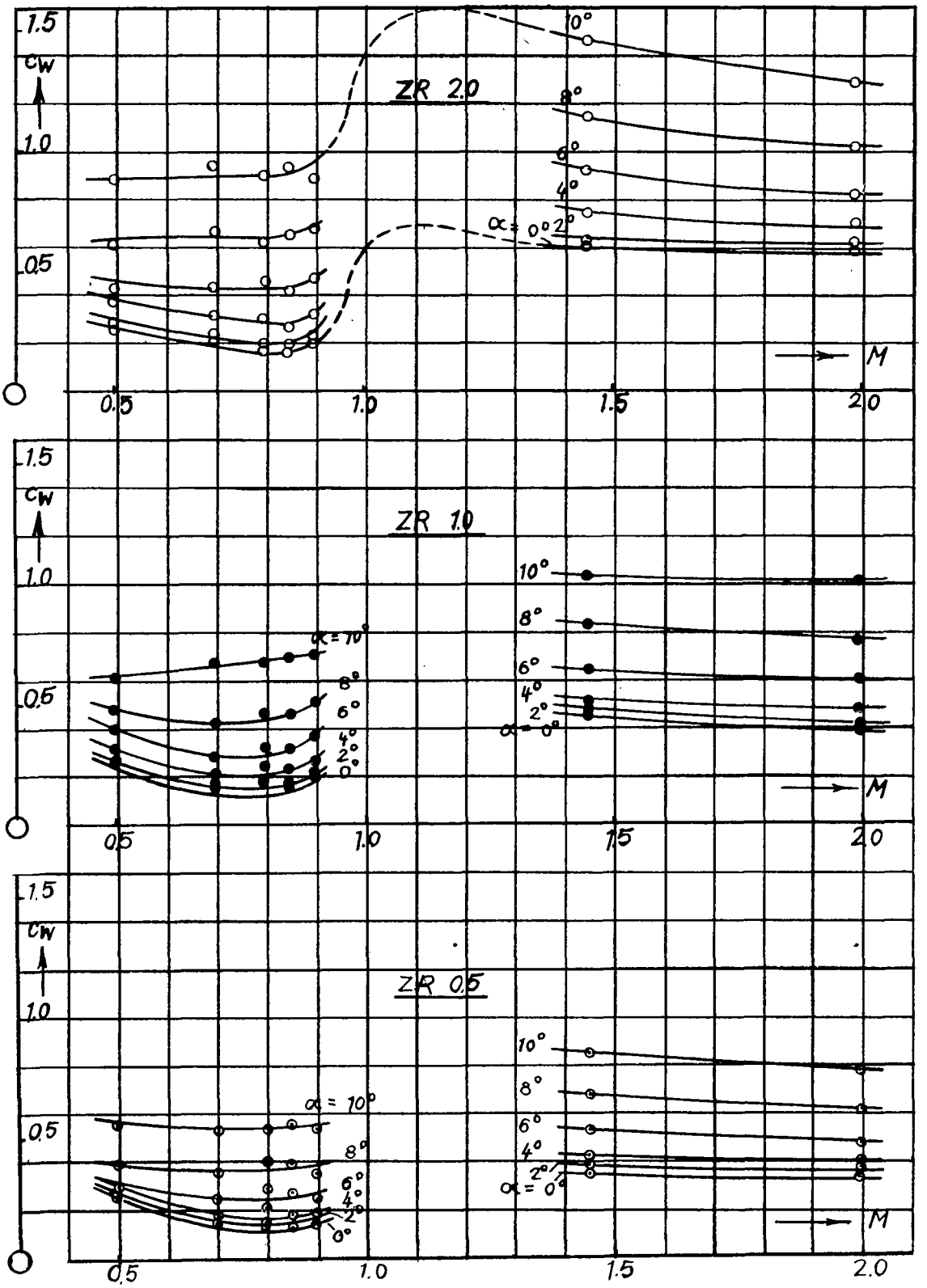

Figure 12.- Drag coefficients.

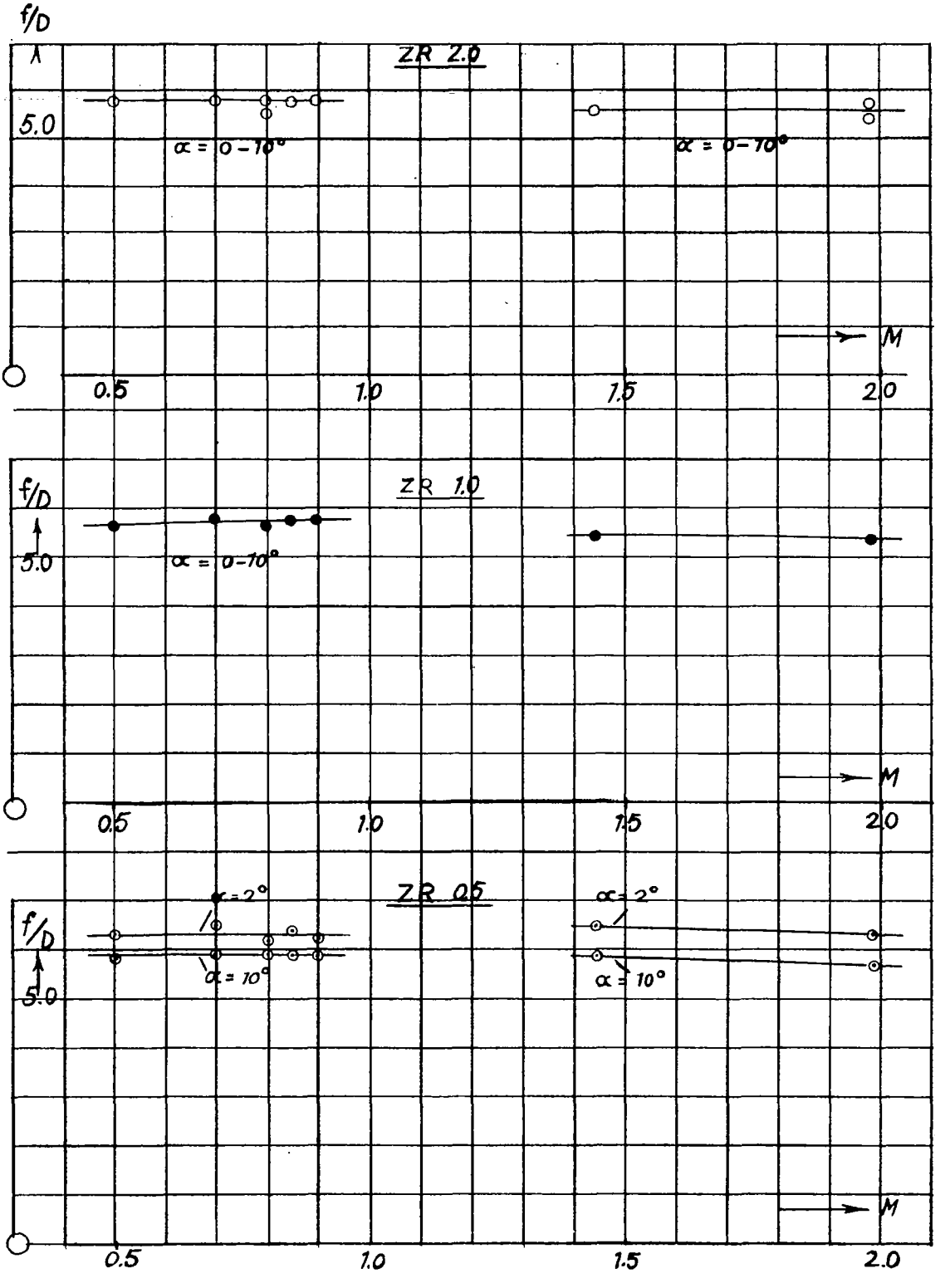

Figure 13.- Positions of the center of pressure point.

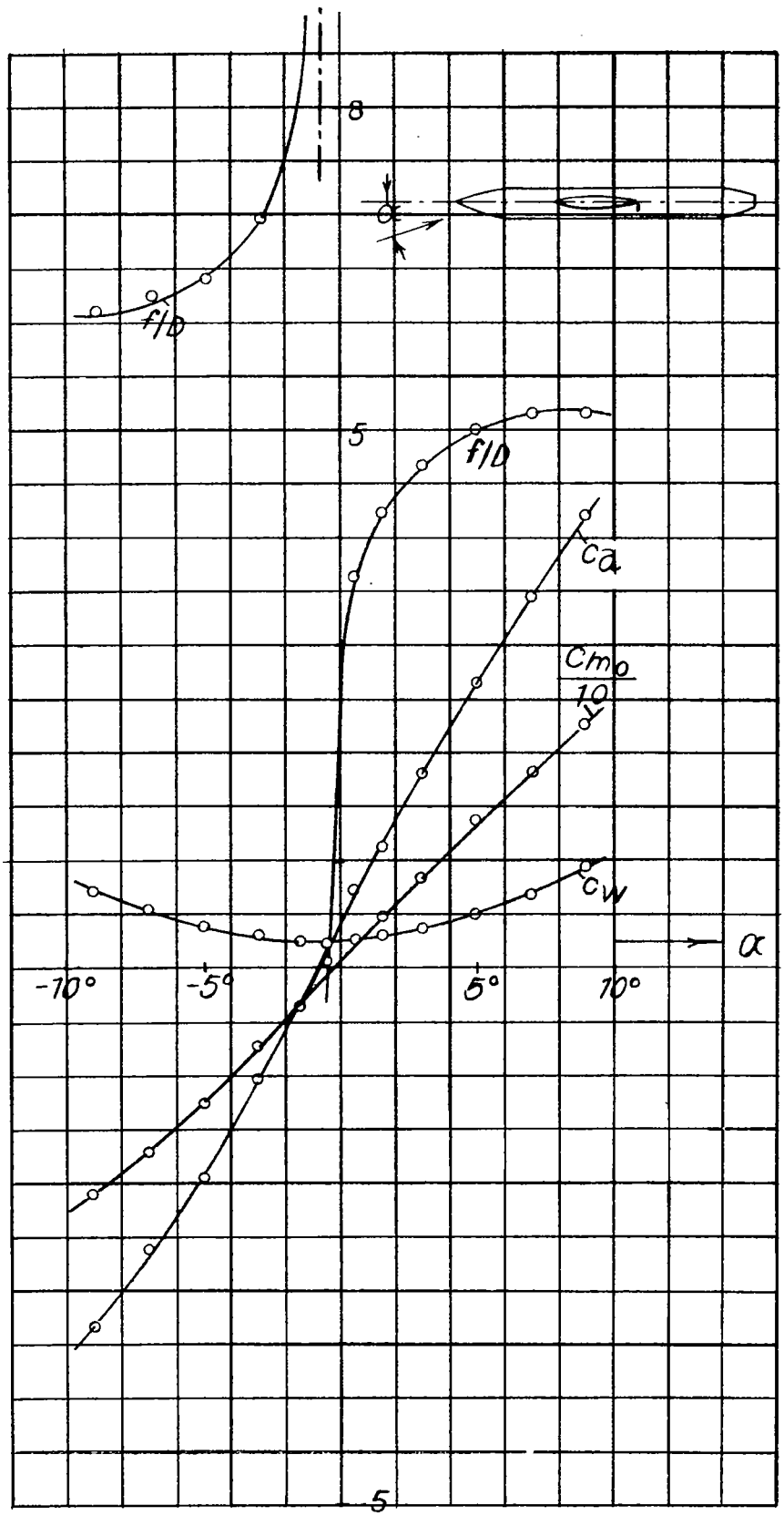

Figure 14.- With deflected rudder ZR 2.0 M = 0.7.

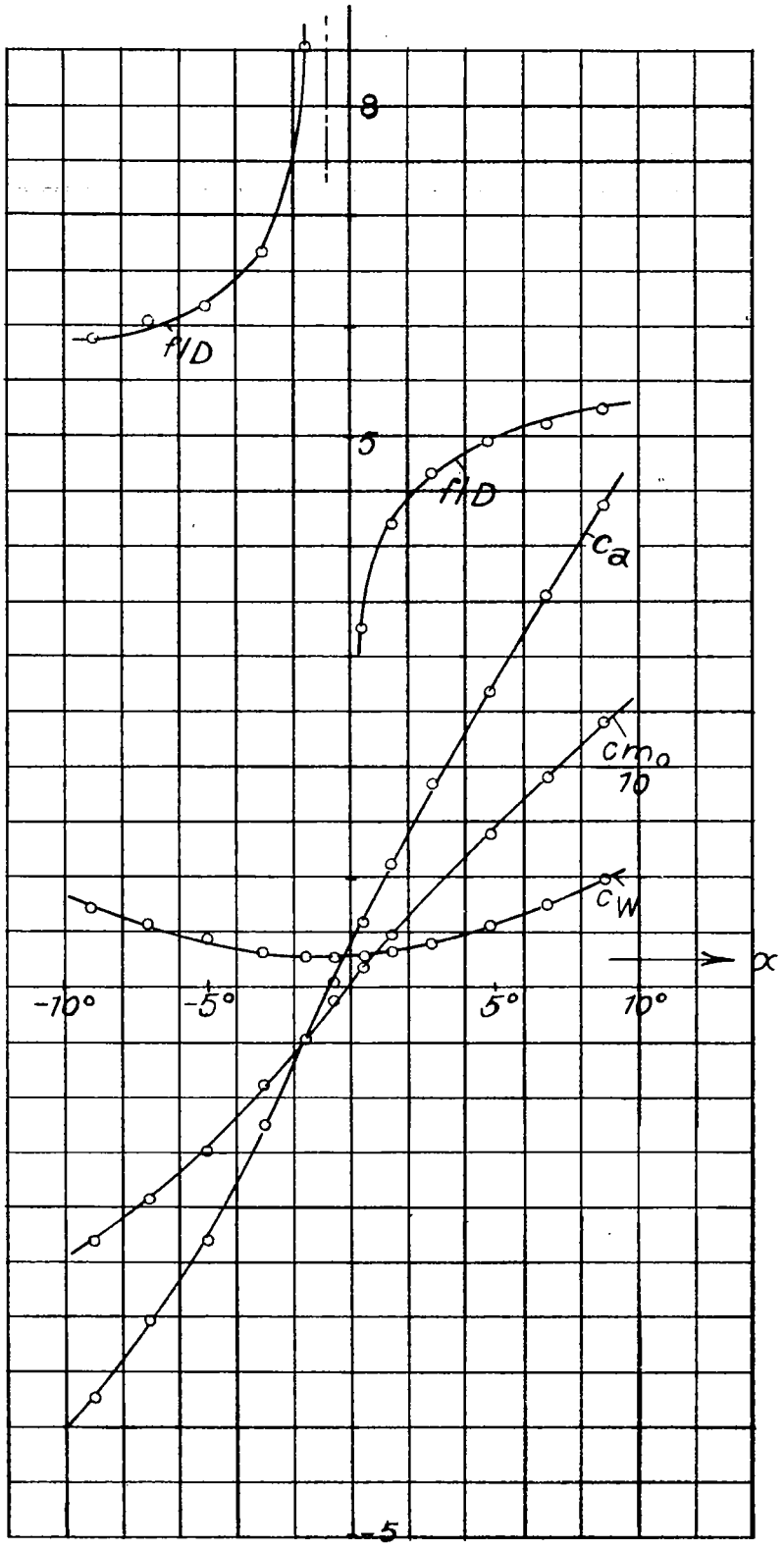

Figure 15.- With deflected rudder ZR 2.0 M = 0.85.

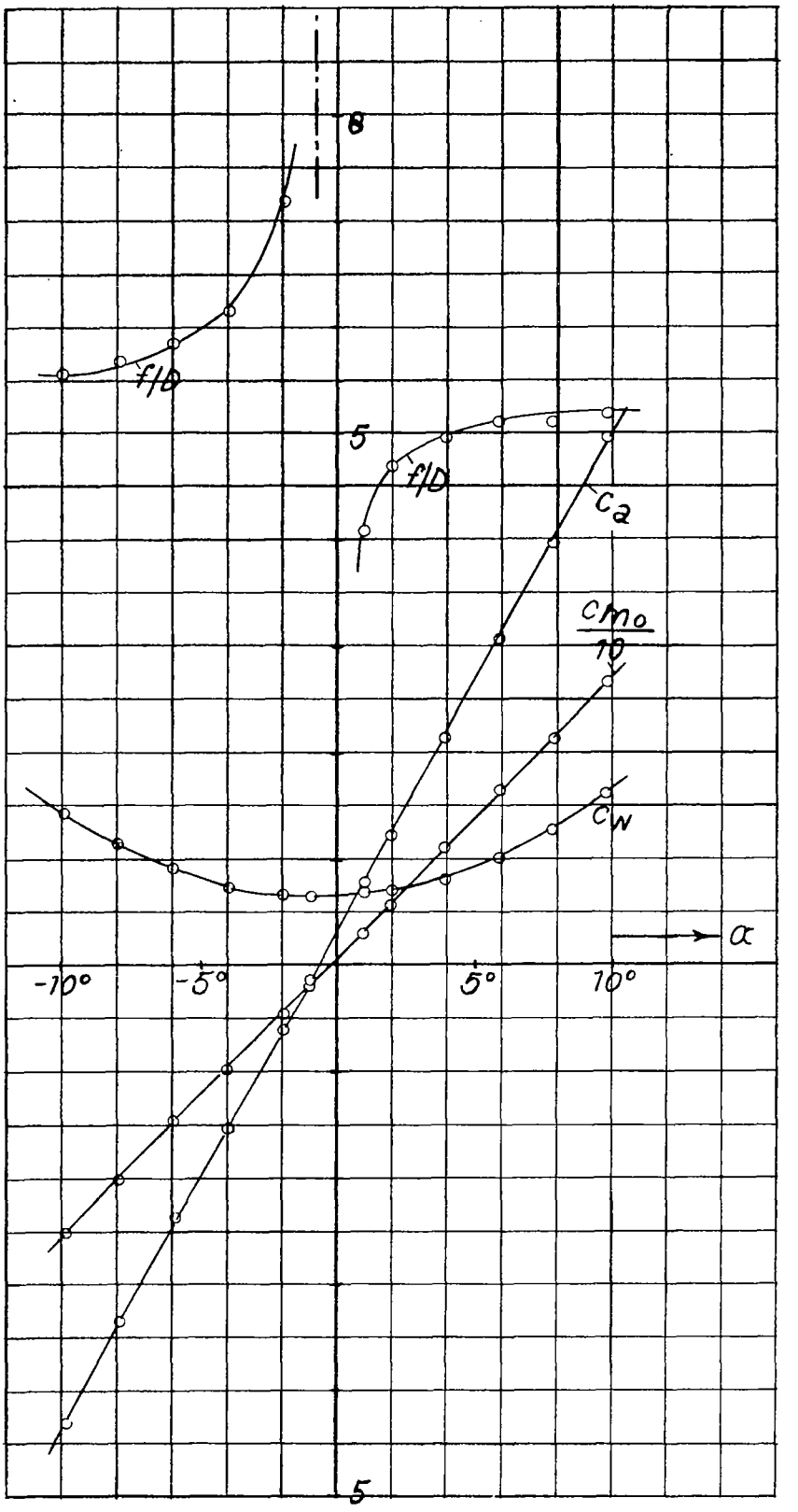

Figure 16.- With deflected rudder ZR 2.0 M = 1.45.

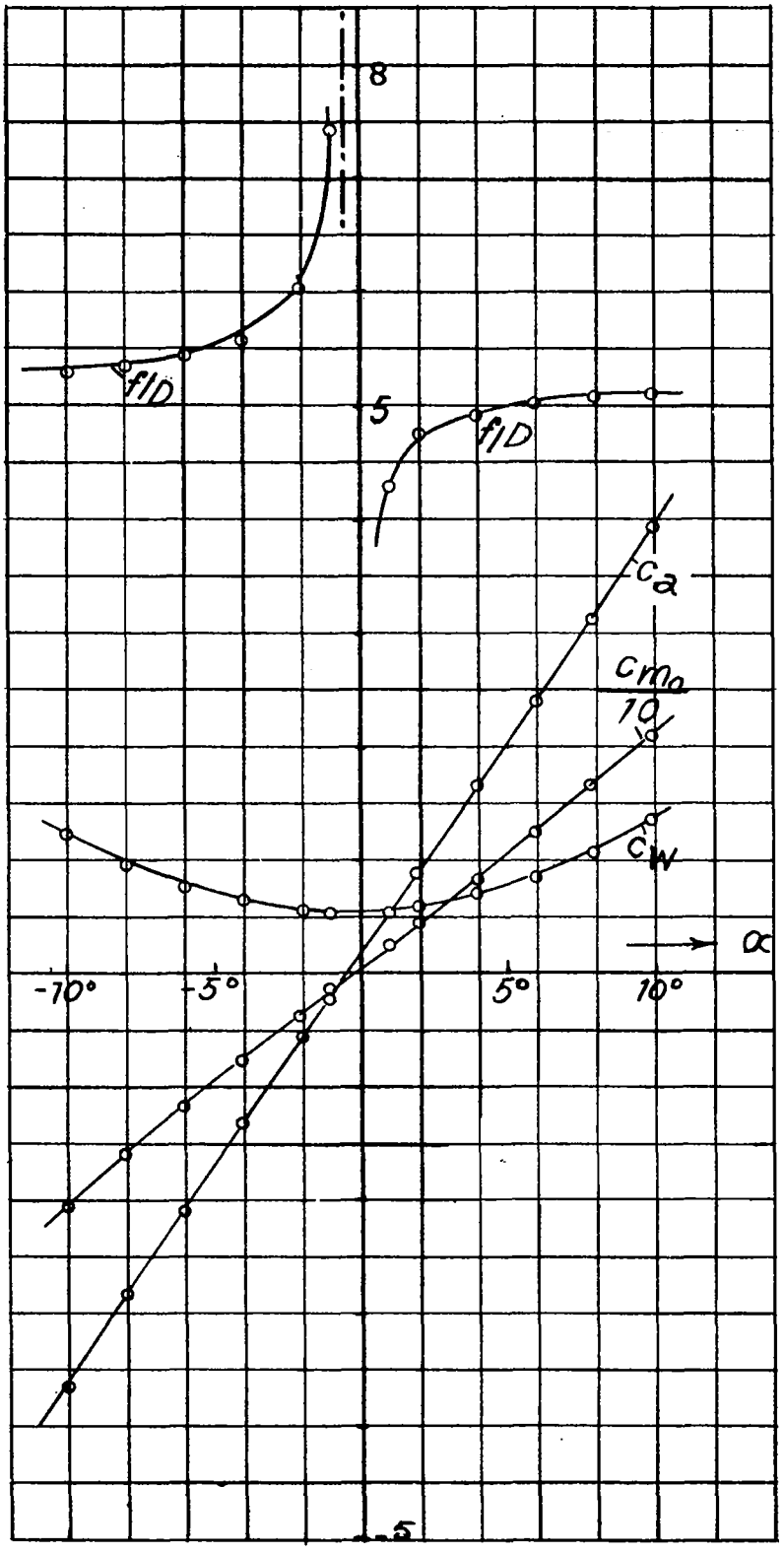

Figure 17.- With deflected rudder ZR 2.0 M = 1.99.

NATIONAL ADVISORY COMMITTEE FOR AERONAUTICS

TECHNICAL MEMORANDUM NO. 1159

WIND-TUNNEL MEASUREMENTS ON THE WING OF THE HENSCHEL MISSILE "ZITTERROCHEN"[1] IN SUBSONIC AND SUPERSONIC VELOCITIES*

By Kehl

Abstract: Supplementing the measured results previously reported, this investigation of three-component measurements on a wing model of the missile "ZR 2.0" was conducted in the subsonic wind tunnel (open-jet 215-millimeter diameter) and in the supersonic wind tunnel (open jet 110 by 130 millimeters) at the request of the Henschel Aircraft Works, Berlin.

Outline: I. Relations and Definitions

II. Description of Model and Measured Results

I. RELATIONS AND DEFINITIONS

A Lift, component of the air force perpendicular to the direction of flow, kilograms

W drag, component of the air forces in the direction of flow, kilograms

---

*"Windkanalmessungen am Flügel des Henschelgerätes 'Zitterrochen' bei Unter- und Überschallgeschwindigkeiten." Zentrale für wissenschaftliches Berichtswesen der Luftfahrtforschung des Generalluftzeugmeisters (ZWB) - Berlin-Adlershof, Untersuchungen und Mitteilungen Nr. 3161. Oct. 24, 1944.

[1]Literally "trembling ray."

M_o moment, referred to the center of the wing leading edge (tail loaded moment positive), meter-kilograms

F wing area, meters^2

b wing span, meters

l wing chord, meters

l_m mean wing chord, meters $\left(\frac{b}{\Lambda}\right)$

ρ air density (kg sec^2 m^{-4})

v stream velocity (m sec^{-1})

a sonic velocity (m sec^{-1})

α angle of attack, degrees

Λ wing aspect ratio $\left(\frac{b^2}{F}\right)$

M Mach number $\left(\frac{v}{a}\right)$

c_a lift coefficient $\left(\frac{A}{\frac{\rho}{2} v^2 F}\right)$

c_w drag coefficient $\left(\frac{W}{\frac{\rho}{2} v^2 F}\right)$

c_{m_o} moment coefficient $\left(\frac{M_o}{\frac{\rho}{2} v^2 F l_m}\right)$

II. DESCRIPTION OF MODEL AND MEASURED RESULTS

In figure 1 the wing under investigation with $\Lambda = 2$ is sketched. The contours are the biconvex profile formed by two circular arcs. The thickness ratio amounts to 6.3 percent. The wing was tested in two directions; these directions A and B are illustrated in figure 1.

The measurements in the subsonic wind tunnel (open-jet 215-millimeter diameter) at $M = 0.5$, 0.7, and 0.85

were taken, as were measurements in the supersonic wind tunnel (open jet 110 by 130 millimeters) at $M = 1.20$, 1.45, and 1.99. Angle of attack ranged from 0° to 10°. The polars and the moment-coefficient curves are given in figures 2 to 5.

For case A, a decrease in the drag was observed with increasing Mach number, just as was formerly noticed on the whole model (see UM 3122), which is traceable to laminar separation at the low Mach numbers. The Reynolds number based upon the mean chord l_m amounts to 3.2×10^5 at $M = 0.5$ and to 4.1×10^5 at $M = 0.85$. In contrast, the case B shows no Reynolds number or Mach number effect on $c_{w_{min}}$ over the same velocity range. In both cases, the lift coefficient increases with Mach number approximately as required by the Prandtl equation.

As was expected, at supersonic velocities the drag coefficient decreased with increasing Mach number at the low values of lift coefficient. Likewise, the lift coefficient decreased with increasing Mach number for a constant angle of attack.

The pressure point in supersonic as well as subsonic flow is independent of Mach number over the range of velocities investigated. In supersonic flow, however, the pressure point lies farther to the rear than in subsonic flow.

Translated by Chance Vought
Aircraft Corporation

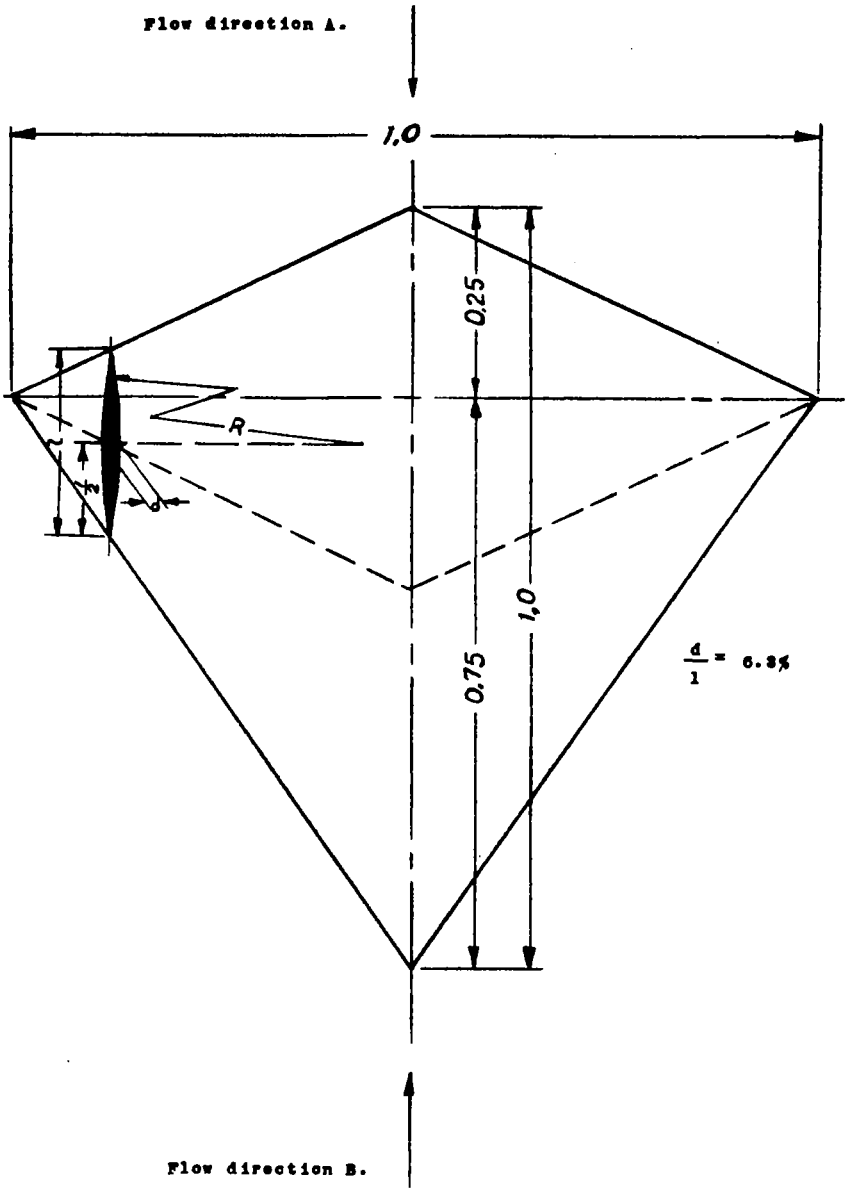

Figure 1.- Wing ZR 2.0; $\Lambda = 2.0$.

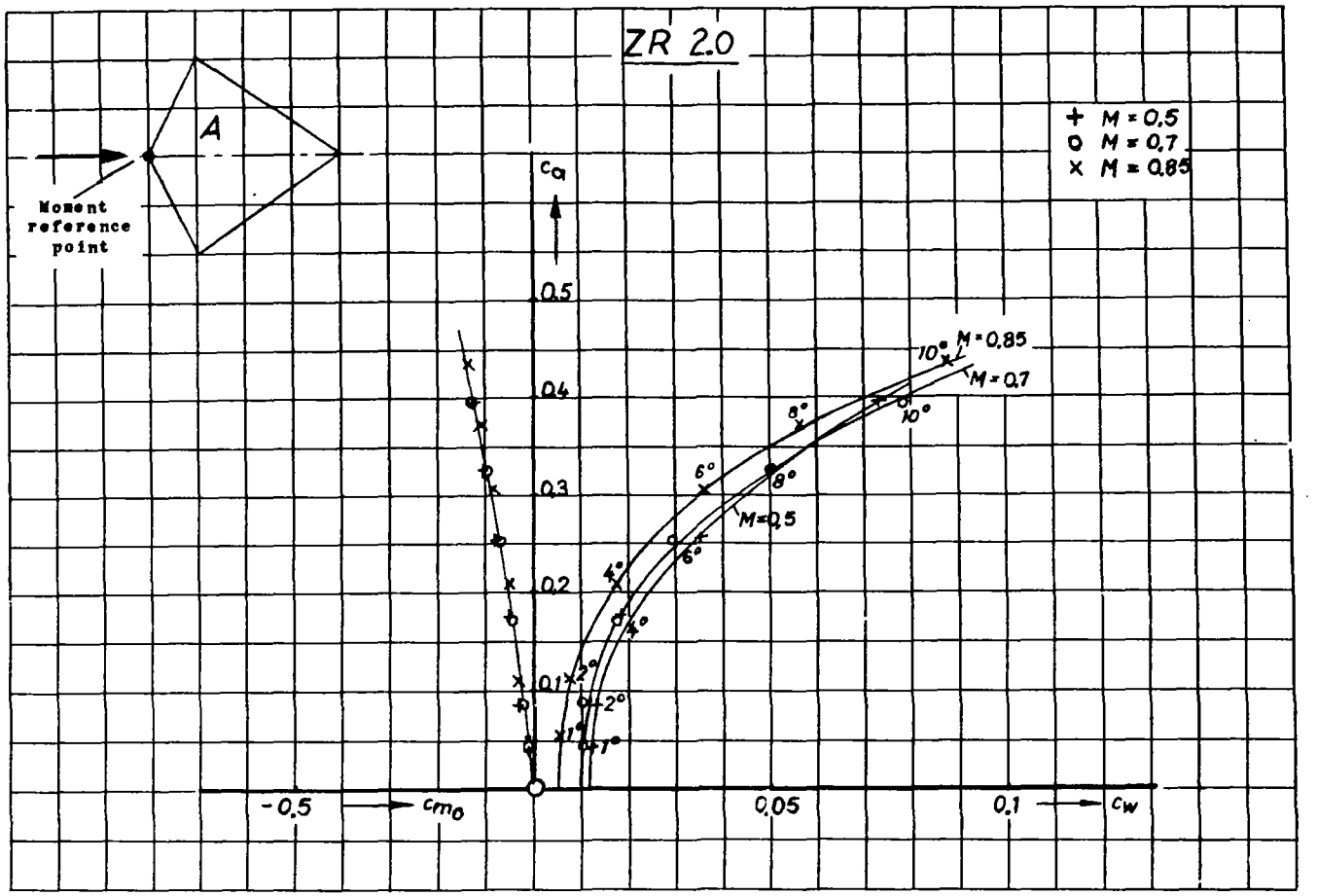
ZR 2.0
A
Moment reference point
+ M = 0.5
o M = 0.7
× M = 0.85
c_a
0.5
0.4
0.3
0.2
0.1
M = 0.85
M = 0.7
M = 0.5
10°
8°
6°
4°
2°
1°
-0.5
c_{m_0}
0.05
0.1
c_w

Figure 2.

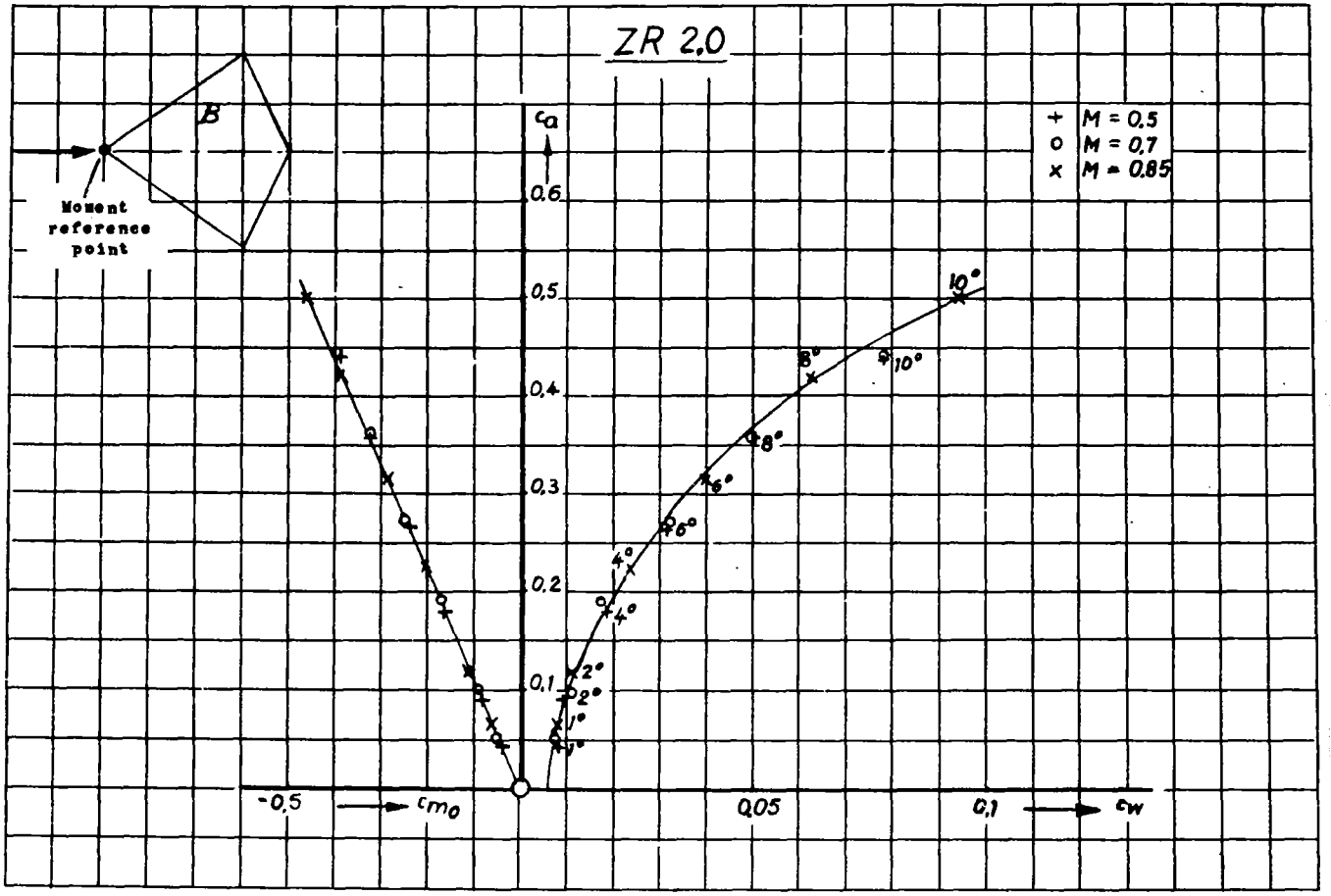
ZR 2.0
B
Moment reference point
c_a
0.6
0.5
0.4
0.3
0.2
0.1
+ M = 0.5
o M = 0.7
× M = 0.85
10°
8°
6°
4°
2°
0°
-0.5
c_{m_0}
0.05
0.1
c_w

Figure 3.

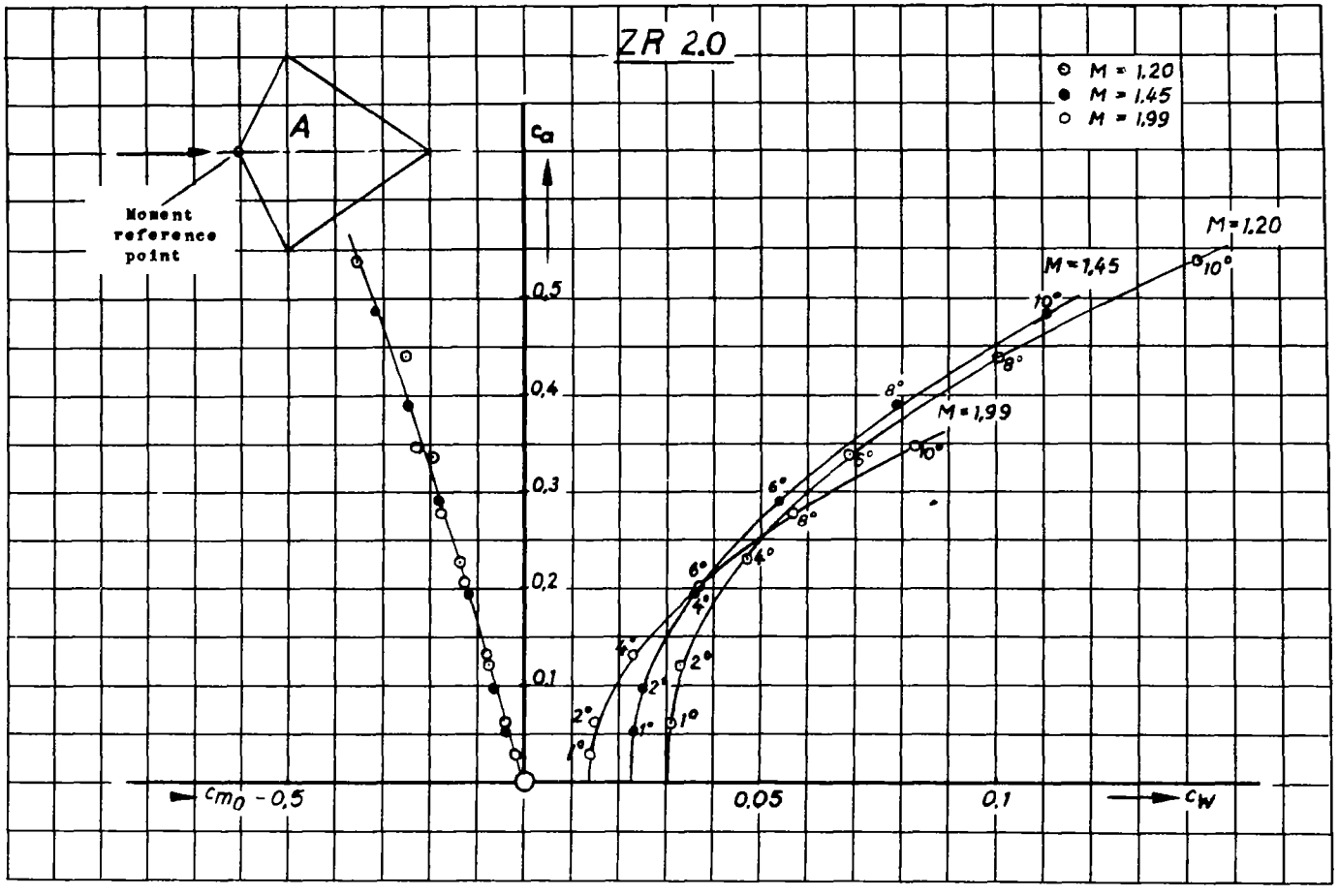
ZR 2.0
M = 1.20
M = 1.45
M = 1.99
A
Moment reference point
c_a
0.5
0.4
0.3
0.2
0.1
M=1.20
M=1.45
M=1.99
$c_{m_0} - 0.5$
0.05
0.1
c_w

Figure 4.

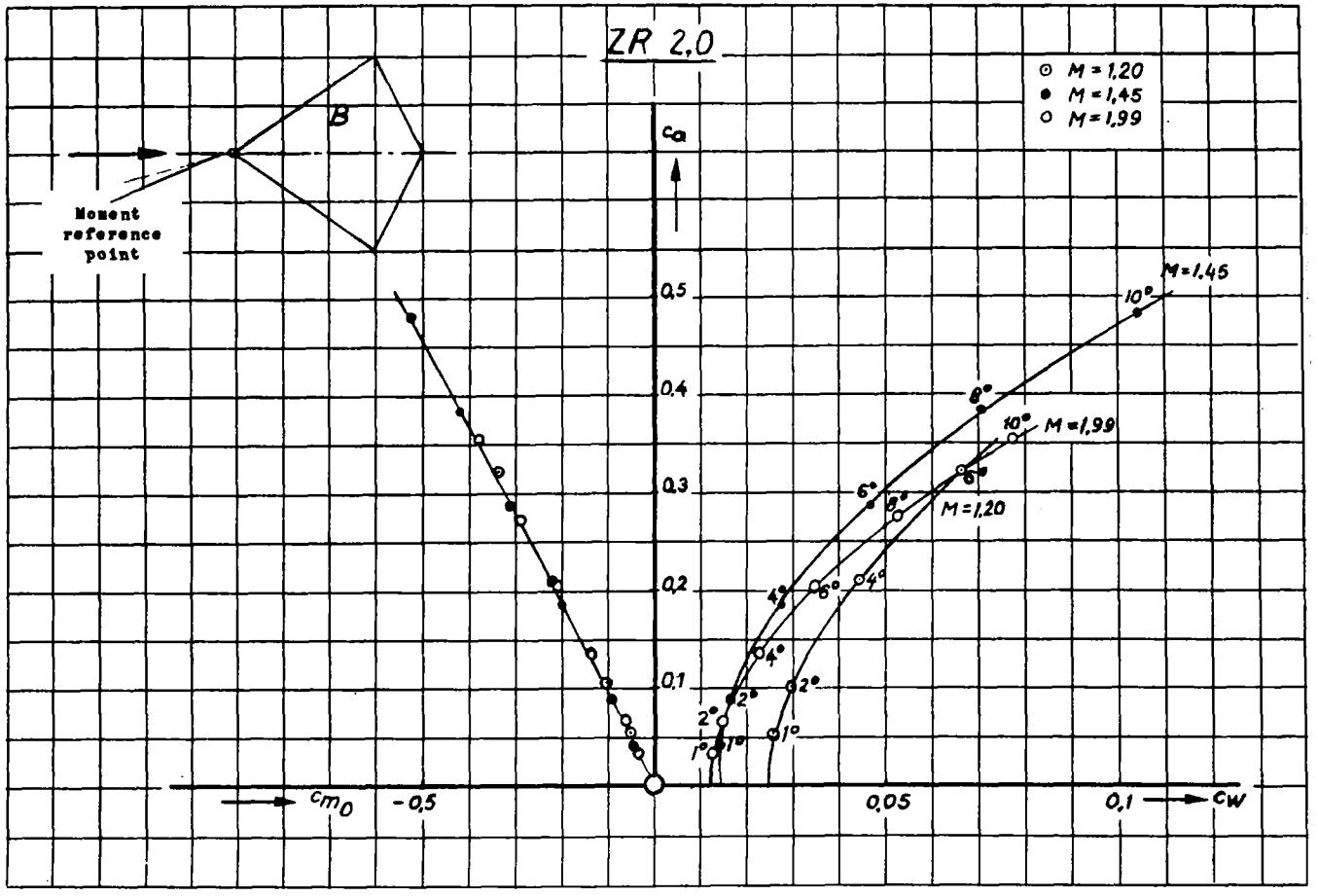
ZR 2,0
B
Moment reference point
M = 1,20
M = 1,45
M = 1,99
c_a
0,5
0,4
0,3
0,2
0,1
M=1,45
10°
8°
10°
M=1,99
6°
8°
6°
M=1,20
4°
6°
4°
4°
2°
2°
2°
1°
1°
1°
c_{m_0}
-0,5
0,05
0,1
c_w

Figure 5.